GEOCHEMISTRY, CLASSIFICATION AND MATURITY OF THE SANDSTONE FACIES OF THE ABEOKUTA FORMATION, SOUTH WESTERN NIGERIA

Madukwe, Henry. Y.
Department of Geology, Ekiti
State University Ado-Ekiti
NIGERIA

Obasi, Romanus. A.
Department of Geology, Ekiti
State University Ado-Ekiti
NIGERIA

ABSTRACT

The geochemistry, classification and maturity of the sandstone facies of the Abeokuta Formation were investigated. A decrease in the abundance of TiO_2, Fe_2O_3, CaO, Na_2O, MgO, MnO, K_2O, and Al_2O_3 as SiO_2 increases was not the trend observed, this could be due to sediment mixing. Arsenic concentration is much higher than that for the UCC which may be due to contamination. Ce, Cu, Pb, V, Y, Zn and Zr were enriched compared with UCC and average sedimentary rocks. The sandstone is extremely depleted in REE (only Ce and Y present) due to dilution effect of quartz. The sandstones exhibited varying classification nomenclatures using different classification schemes, which may be due to sediment supply from different sources. However, the sandstones are rich in iron, potassic and rich in lithic materials--they can thus be classified as litharenites and sub-arkoses. The sandstones have a low SiO_2/Al_2O_3 value (avg. 7) suggesting chemical immaturity; high degree of clayness and less calcified. The high Fe_2O_3/K_2O ratio (avg. 13) with low SiO_2/Al_2O_3 ratio shows that they are mineralogically less stable and more prone to reactivity during supercritical CO_2 exposure. The alkali content indicates the presence of feldspars and low chemical maturity. Index of compositional variation (ICV) values shows that the sandstones are mineralogically immature. The plot of ratio SiO_2/Al_2O_3 against quartz / (feldspar + lithic fragments) shows that the sandstones are immature. The ZTR indices suggest that nearly all the sediments are mineralogically immature to sub mature but the mineralogical maturity index classifies the sediments as sub mature to super mature. On the Al—Ti—Zr diagram, the sandstones plotted in the CAS zone and outside all fields with a limited range of TiO_2/Zr variations, suggesting poor sorting and rapid deposition.

Keywords: Abeokuta Formation, sandstones, maturity, classification.

INTRODUCTION

Sediments are loose, solid particles that originate from the weathering and erosion of pre-existing rocks (igneous, metamorphic and sedimentary) and the chemical precipitation from solution including secretion by organisms in water. These sediments are then transported sorted, deposited and lithified to form sedimentary rocks. Sedimentary rocks are classified into clastic and non-clastic. The clastic are also classified into terrigenous clastics and volcaniclastics. The terrigenous clastics sedimentary rocks are further categorized into mudrocks, sandstones and conglomerates (Nichols, 2009). Sand may be defined as a sediment consisting primarily of grains in the size range 63 μm to 2mm and a sandstone is defined as a sedimentary rock with grains of these sizes. This size range is divided into five intervals: very fine, fine, medium, coarse and very coarse (Nichols, 2009). The evolution of the Dahomey Basin (Figure 1) is generally believed to be due to rifting phenomenon associated with the separation of the mega-continent called Gondwanaland. According to Agagu (1985) the stratigraphy in most parts of the basin is dominated by alternating sands and shales with minor proportion of limestone. This study intends to classify the sandstone

facies of Abeokuta Formation exposed at Irolu and J4 Reserve Area, southwestern Nigeria based on geochemistry and mineralogy.

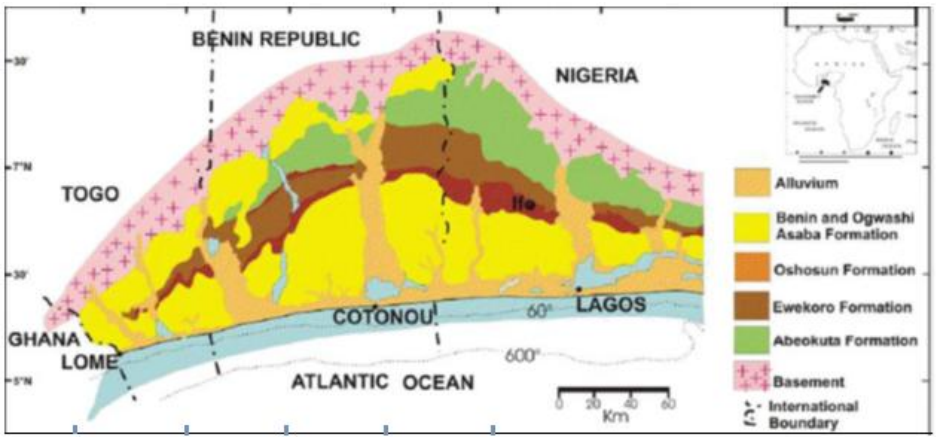

Figure 1: Geological Map of the Dahomey Basin (Bankole *et al*., 2005)

GEOLOGIC SETTING AND STRATIGRAPHY

Detailed stratigraphy of the Basin has been delineated by several workers (Jones and Hockey, 1964; Adegoke, 1969; Ogbe, 1970; Billman, 1976; Ako et al., 1980; Omatsola and Adegoke, 1981; Okosun, 1990). However, there is still no unified stratigraphic system for the basin; there are still geological polemics about age and lithological classifications. Table 1 shows the lithostratigraphy from the oldest to the youngest according to Jones and Hockey, 1964; Omatsola and Adegoke, 1981; Agagu, 1995: the Cretaceous Abeokuta Group—made up of the Ise formation, Afowo formation and Araromi formation. Shallow marine Paleocene Ewekoro Formation deposited during transgressive episode overlies the Abeokuta Group. The Ewekoro formation is widespread covering a distance of about 32km from Ghana, eastwards towards the eastern margin of the basin. It finally becomes fine grained into the dominantly shelly Araromi formation which pinches out against the Western flank of Okitipupa ridge (Adegoke, 1969, 1977). Akinbo Formation (Paleocene-Eocene) overlies the Ewekoro Formation. The Eocene Oshosun Formation overlies the Akinbo Formation and Oshosun Formation is overlain by the regressive arenaceous Ilaro Formation. Figure 2 is a geological map showing the study area and the sample location.

Table1. Stratigraphy of the Benin Basin

PERIOD	Jones & Hockey (1964)		Adegoke & Omatsola (1981)		Agagu (1995)	
	Age	Formation	Age	Formation	Age	Formation
Quaternary	Recent	Alluvium			Recent	Alluvium
Tertiary	Pleistocene – Oligocene	Coastal Plain Sand	Pleistocene – Oligocene	Coastal Plain Sand	Pleistocene – Oligocene	Coastal Plain Sand
	Eocene	Ilaro sandstone	Eocene	Ilaro sandstone/Oshosun shales	Eocene	Ilaro sandstone/Oshosun shales
	Paleocene	Ewekoro Limestone	Paleocene	Akimbo shale/Ewekoro Limestone	Paleocene	Akimbo shale/Ewekoro Limestone
Late Cretaceous	Late Senonian	Abeokuta Formation	Maastrichtian to Neocomian	Araromi shale Afowo sandstone/shale	Maastrichtian to Neocomian	Araromi shale Afowo sandstone/shale
				Ise sandstone		Ise sandstone
Precambrian Basement Complex						

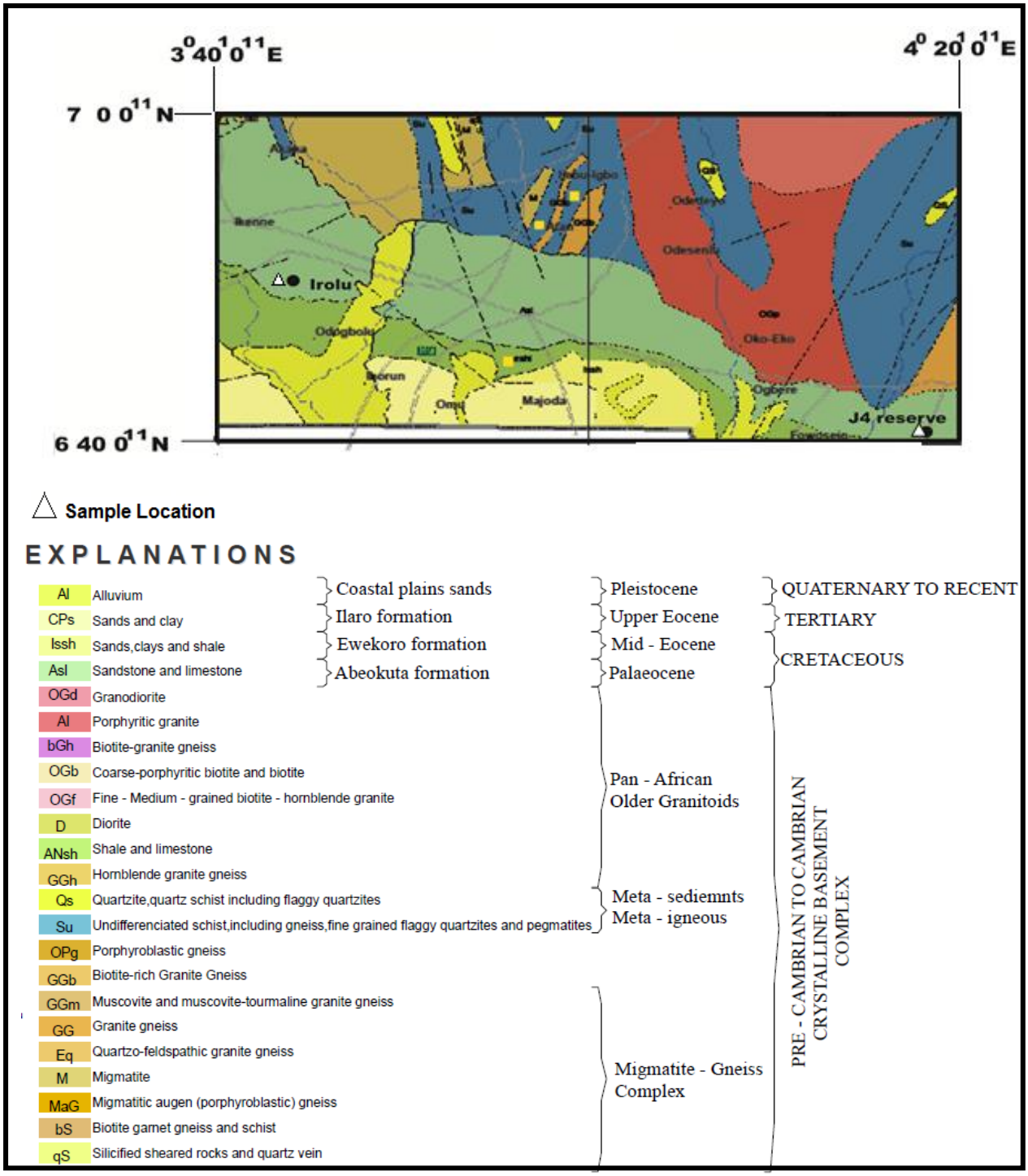

Figure 2: The study area and sample location, modified from Nigerian Geological Survey Agency (2009

METHODOLOGY

Fourteen (14) samples were analyzed for major oxides, trace and rare earth elements using X-Ray Fluorescence (XRF) and LA-ICP-MS at Stellenbosch University, South Africa. Pulverised sandstone samples were analysed for major element using Axios instrument (PANalytical) with a 2.4 kWatt Rh X-ray Tube. The detailed procedures for sample preparation for the analytical technique are reported below.
Fusion bead method for Major element analysis:

- Weigh 1.0000 g ± 0.0009 g of milled sample
- Place in oven at 110 ºC for 1 hour to determine H_2O^+
- Place in oven at 1000 ºC for 1 hour to determine LOI
- Add 10.0000 g ± 0.0009 g Claisse flux and fuse in M4 Claisse fluxer for 23 minutes.
- 0.2 g of $NaCO_3$ was added to the mix and the sample+flux+$NaCO_3$ was pre-oxidized at
- 700 °C before fusion.
- Flux type: Ultrapure Fused Anhydrous Li-Tetraborate-Li-Metaborate flux (66.67 % $Li_2B_4O_7$ + 32.83 % $LiBO_2$) and a releasing agent Li-Iodide (0.5 % LiI).

The result returned eleven major elements, reported as oxide percent by weight (SiO_2, TiO_2, Al_2O_3, Fe_2O_3, MgO, MnO, CaO, Na_2O, K_2O, SO_3 and P_2O_5). Loss on Ignition (LOI) is a test used in XRF major element analysis which consists of strongly heating a sample of the material at a specified temperature, allowing volatile substances to escape or oxygen is added, until its mass ceases to change. The LOI is made of contributions from the volatile compounds of H_2O^+, OH^-, CO_2, F^-, Cl^-, S; in parts also K^+ and Na^+ (if heated for too long); or alternatively added compounds O_2 (oxidation, e.g. FeO to Fe_2O_3), later CO_2 (CaO to $CaCO_3$). In pyro-processing and the mineral industries such as lime, calcined bauxite, refractories or cement manufacturing industry, the loss on ignition of the raw material is roughly equivalent to the loss in mass that it will undergo in a kiln, furnace or smelter.

The trace and rare elemental data for this work was acquired using Laser Ablation-inductively coupled plasma spectrometry (LA-ICP-MS) analyses. The analytical procedures are as follows:

Pulverised sandstone samples were analysed for trace element using LA-ICP-MS instrumental analysis. LA-ICP-MS is a powerful and sensitive analytical technique for multi-elemental analysis. The laser was used to vaporize the surface of the solid sample, while the vapour, and any particles, were then transported by the carrier gas flow to the ICP-MS. The detailed procedures for sample preparation for both analytical techniques are reported below.
Pressed pellet method for Trace element analysis

- Weigh 8 g ± 0.05 g of milled powder
- Mix thoroughly with 3 drops of Mowiol wax binder
- Press pellet with pill press to 15 ton pressure
- Dry in oven at 100 ºC for half an hour before analysing.

The analysis yielded thirteen Trace elements and two Rare Earth elements: As, Ba, Ce, Co, Cu, Nb, Ni, Ti, Pb, Rb, Sr, V, Y, Zn, and Zr reported as mg/kg (ppm).

RESULTS AND DISCUSSION

Classification

The concentrations of three major oxide groups have been used to classify sandstones: silica and alumina, alkali oxides, and iron oxide plus magnesia. Blatt et al., (1972), Pettijohn et al., (1972) and Herron (1988) examined the importance of these major oxide variables.

Table 2: The chemical composition of Abeokuta Formation and weathering indices (major oxides expressed in percentages (%), trace and REE in parts per million (ppm)

Elements	Irolu 1	Irolu 2	Irolu 3	Irolu 5	Irolu 6	Irolu 7	Irolu 8	Irolu 9	Irolu 10	Irolu 11	Irolu 12	J4-1	J4-2	J4-3
SiO_2	63.08	62.91	71.66	57.24	60.79	60.58	60.5	53.38	70.64	43.83	56.44	60.34	64.6	55.3
Al_2O_3	9.14	8.37	6.88	13.52	12.5	8.43	8.53	8.36	6.05	3.62	13.84	10.78	8.37	6.93
Fe_2O_3	15.35	16.57	9.21	12.59	12.26	19.18	19.24	26.09	13.03	10.49	12.46	18.27	15.6	25.6
MnO	0.08	0.15	0.07	0.06	0.05	0.18	0.18	0.3	0.09	0.47	0.07	0.11	0.13	0.25
MgO	1.56	1.58	0.98	1.93	1.89	2.61	2.53	2.55	1.21	0.61	1.87	2.36	2.19	1.87
CaO	0.85	1.22	2.5	0.42	0.49	1.61	1.61	2.17	2.27	28.88	0.8	0.93	1.22	2.49
Na_2O	1.54	1.39	1.43	0.78	1.17	1.66	1.67	1.37	1.22	1.41	0.9	1.83	1.87	1.67
K_2O	3.34	2.72	1.97	6	3.83	0.83	0.83	0.93	0.92	0.49	4.52	1.2	1.08	1.59
TiO_2	3.15	2.74	1.8	1.43	1.47	1.78	1.78	1.18	2.21	0.83	1.46	1.6	2.1	3.23
P_2O_5	0.2	0.16	0.16	0.11	0.13	0.22	0.22	0.22	0.21	0.11	0.13	0.19	0.2	0.23
SO_3	0.11	0.09	0.23	0.2	0.18	0.06	0.06	0.08	0.05	0.02	0.25	0.03	0.04	0.13
As	215	230	144	154	102	155	154	263	166	216	103	174	138	330
Ba	452	333	179	593	385	197	217	244	177	194	634	138	200	331
Ce	146	173	99	171	179	84	118	180	111	269	211	91	109	172
Co	14	9	19	14	8	24	15	12	8	6	18	16	16	16
Cu	52	55	37	50	54	54	53	63	52	66	72	56	51	81
Nb	8	9	8	29	24	7	5	10	17	19	23	14	13	19
Ni	20	22	22	32	27	18	32	28	27	29	43	32	24	36
Pb	12	36	35	90	41	13	13	19	38	3	62	25	11	21
Rb	64	64	47	311	151	26	26	28	30	12	264	39	28	43
Sr	92	96	121	199	167	68	68	82	85	746	199	90	90	805
V	52	96	78	127	121	108	118	129	107	217	174	150	131	138
Y	21	25	20	36	39	27	24	26	18	34	45	21	22	36
Zn	88	74	64	116	91	70	68	88	63	53	112	61	82	74
Zr	480	559	365	276	400	227	228	194	183	136	264	251	303	213

The classification schemes used are the geochemical classification diagrams of Pettijohn *et al.*, (1972); Blatt et al., (1972); Folk (1974); Herron (1988); and the geochemical classification of Lindsey, (1999). Figure 3 (Folk. 1974) classified the Abeokuta sandstone facies as quartzarenites with some sublitharenite and subarkose indicating that they are slightly mineralogically mature. The geochemical classification diagram (Figure 4) by Herron (1988) classifies them mainly as Fe-sands with little portions on the wacke zone. High MgO or Fe_2O_3 will yield anomalously high $(Fe_2O_3+MgO)/(K_2O+Na_2O)$, causing the sample to plot outside the compositional fields for other sandstones (Lindsey, 1999). Pettijohn *et al.* (1972) classification scheme for these sandstones (Figure 5) shows that they plotted mainly in the litharenite field and few on the arkose field.

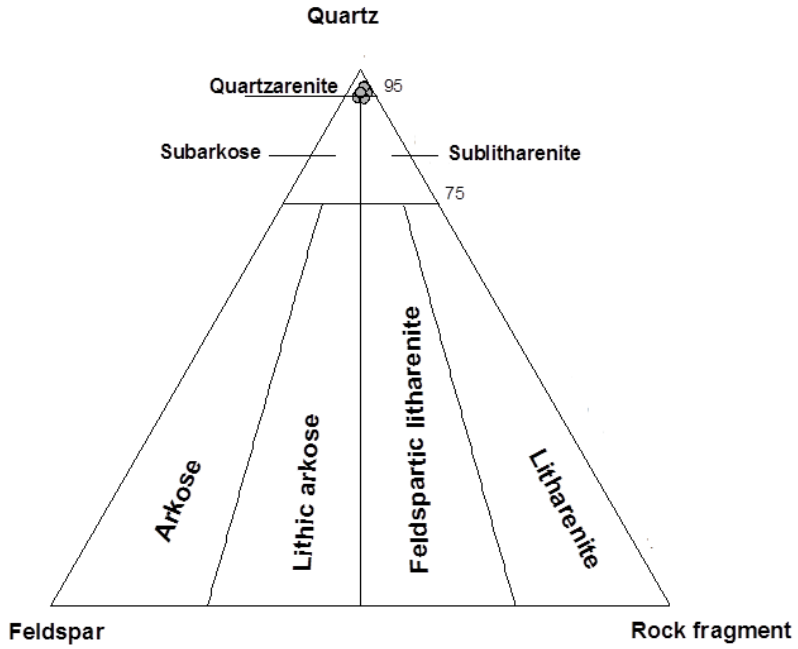

Figure 3: QFL ternary classification plot (Folk, 1974) of the Abeokuta sandstone facies.

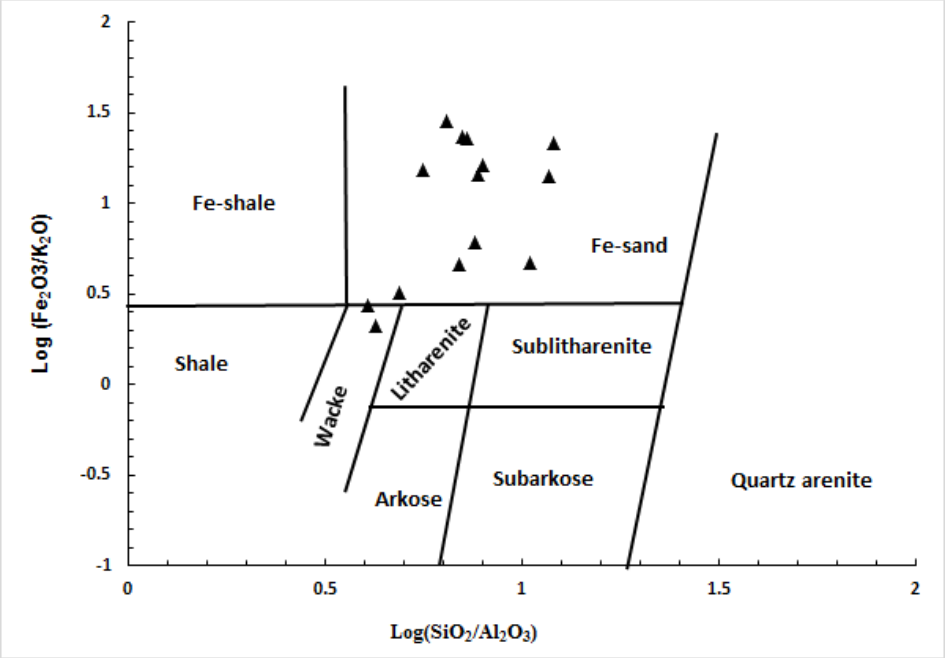

Figure 4. Chemical classification of the Abeokuta FM based on log (SiO_2/Al_2O_3) *vs.* log (Fe_2O_3/K_2O) diagram of Herron (1988).

Using the ternary diagram proposed by Blatt et al., (1972), the Abeokuta sandstone facies plotted mainly in ferromagnesian potassic sandstones field with minor occurrence in the sodic field (Figure 6). The ternary diagram by Blatt et al., (1972) omitted sandstones with less than 5% Al2O3, consequently, quartz arenites is missing. Based on the work by Lindsey (1999) using data from Pettijohn (1963; 1975), average lithic arenites plotted in the ferromagnesian Potassic sandstones field, average greywacke plotted in the sodic sandstone field while average arkose appeared in the potassic sandstones field. According to Pettijohn, (1963), the lithic arenites are a diverse and poorly defined class. In addition to abundant rock fragments

of widely varying composition, many lithic arenites contain clay matrix with different compositions which can contain higher levels of Fe and Mg. Also, many rock fragments of lithic sandstones are composed of materials that vary greatly in composition.

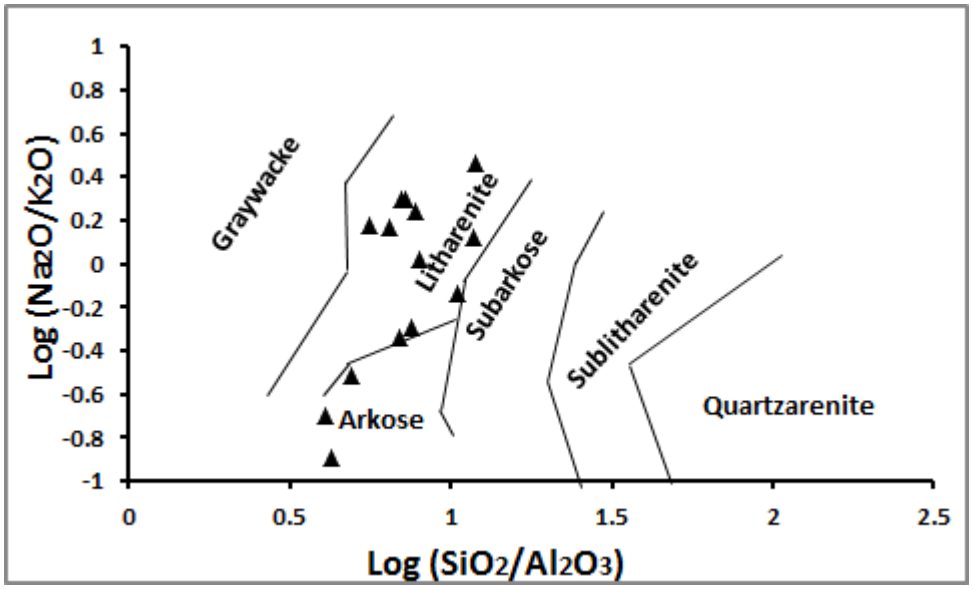

Figure 5. Chemical classification of the Abeokuta Formation based on log (SiO_2/Al_2O_3) *vs.* log (Na_2O/K_2O) diagram of Pettijohn *et al.* (1972)

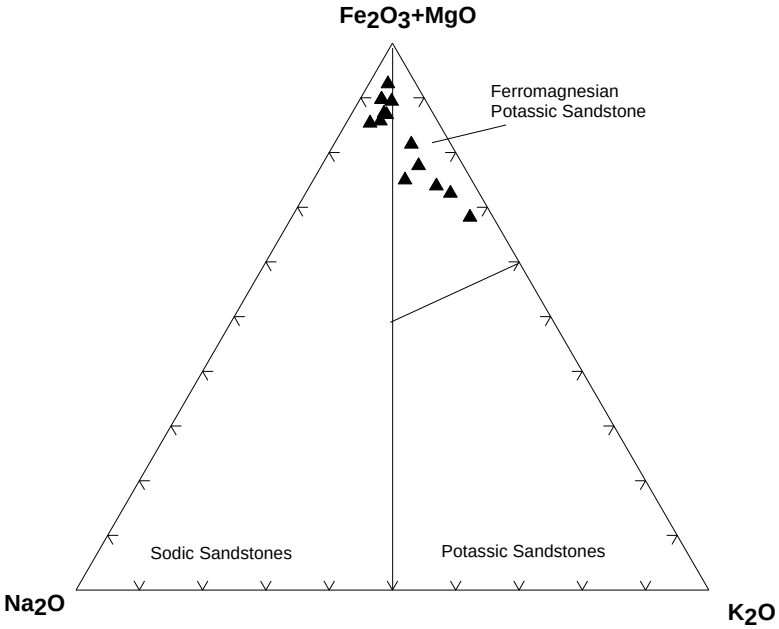

Figure 6: Ternary diagram of Na_2O-K_2O-(Fe_2O_3+MgO) from Blatt et al., (1972).

Based on compositional fields for major classes of sandstones (Lindsey, 1999), the sandstones plotted in the greywacke and arkose fields (Figures 7) and lithic arenite field (Figures 8).

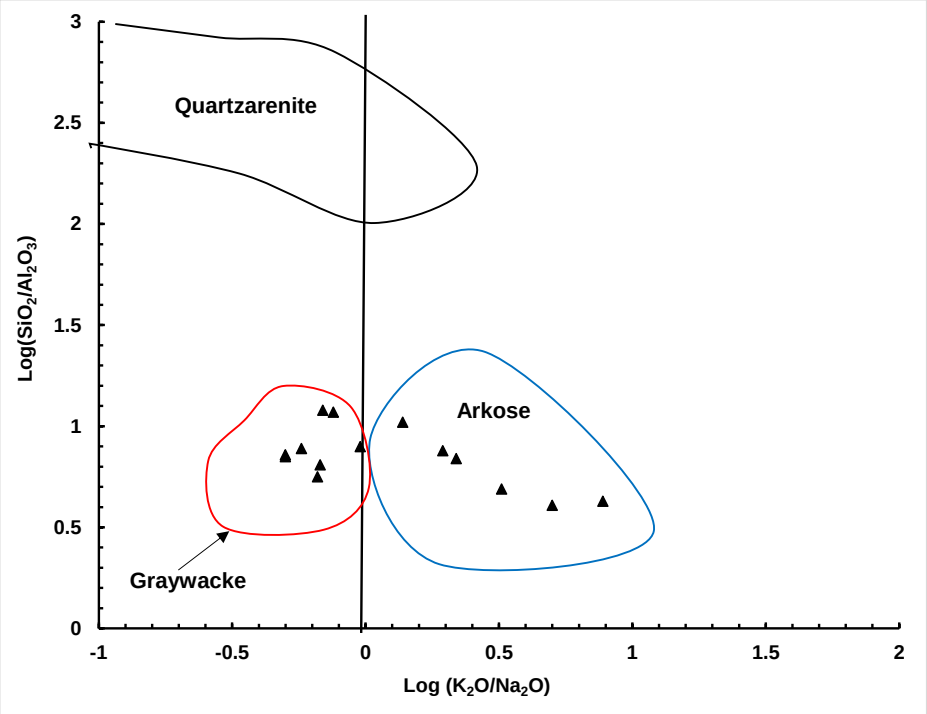

Figure 7: Compositional fields for major classes of sandstones based on data from Pettijohn (1963; 1975): log (SiO_2/Al_2O_3) vs log (K_2O/Na_2O). Abeokuta sandstone facies plotted in the greywacke and arkose fields (adapted from Lindsey, 1999).

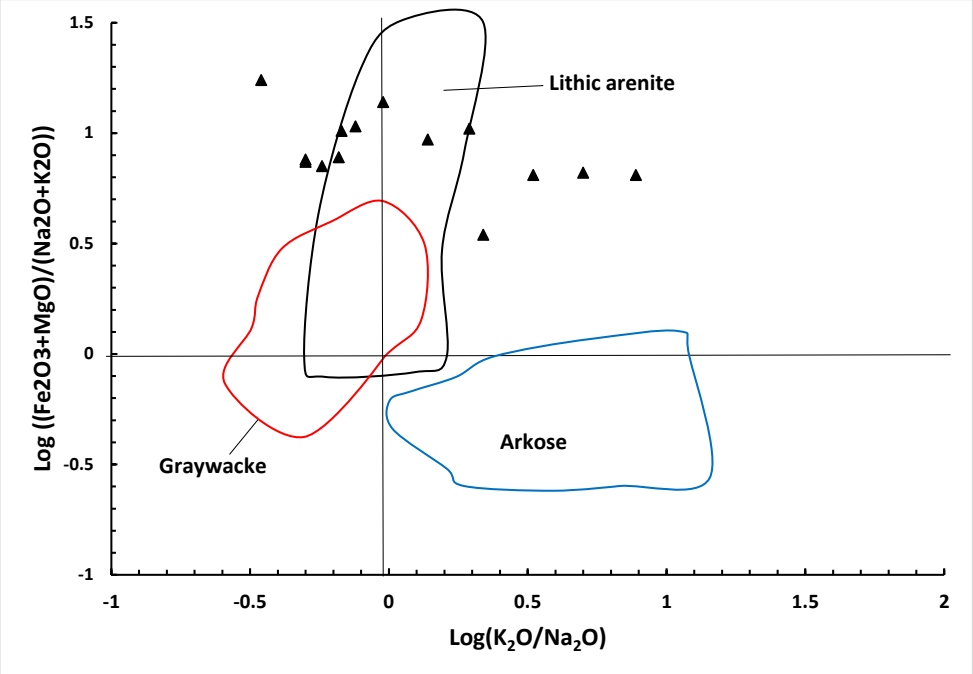

Figure 8: Compositional fields for major classes of sandstones based on data from Pettijohn (1963; 1975): log ((Fe_2O_3+MgO)/(K_2O+Na_2O)) vs log (K_2O/Na_2O). Abeokuta sandstone facies plotted in the lithic arenite field with some falling outside all the fields (adapted from Lindsey, 1999).

Based on the study of a reference set, Lindsey (1999) proposed the following guidelines for chemical classification of sandstones:

1) quartz arenite: log (SiO_2/Al_2O_3) ≥ 1.5

2) graywacke: log ($SiO_2/Al2O_3$) < 1 and log (K_2O/Na_2O) < 0
3) arkose (includes subarkose): log ($SiO_2/Al2O_3$) < 1.5 and log (K_2O/Na_2O) ≥ 0 and log ((Fe_2O_3+MgO)/(K_2O+Na_2O)) < 0
4) lithic arenite (subgraywacke, includes protoquartzite): log ($SiO_2/Al2O_3$) < 1.5 and either log (K_2O/Na_20) < 0 or log ((Fe_2O_3+MgO)/(K_2O+Na_2O)) ≥ 0. If log (K_2O/Na_2O) < 0, lithic arenite can be confused with graywacke.

The sandstone facies of the Abeokuta Formation falls within the requirements of the fourth condition and thus classifies as a lithic arenite.

Maturity

Maturity can be reflected in finer grain sizes; however it is actually clay content that is more directly related to lack of maturity. Maturity is reflected best in quartz, rock fragments, feldspars and grain size. As the percentage of quartz increases the mineralogical maturity does too. Sandstones usually contain clay minerals growing on the surface of the grains or linning and sometimes filling the pore space (Prothero, 2004). The distribution of these clay minerals in sandstone is a key to understanding their properties such as porosity and ultimately, behaviour as hydrocarbon reservoirs (Prothero, 2004). The low values given from the ratio of SiO_2/Al_2O_3 indicate that all the samples have high degree of clayness, which can suggest mineralogical immaturity. Maturity of sandstones can be reflected by the SiO_2/Al_2O_3 index. High ratios indicate mineralogically mature (quartzose, rounded) samples, while low ratios represent chemically immature samples (Potter, 1978). SiO_2/Al_2O_3 ratios of clastic rocks are sensitive to sediment recycling and weathering process and can be used as an indicator of sediment maturity. With increasing sediment maturity, quartz survives preferentially to feldspars, mafic minerals and lithics (Roser and Korsch, 1986; Roser et al., 1996). The sandstones have SiO_2/Al_2O_3 ratios of between 4 and 12 (average = 7), this low ratios represents chemically immature samples. Na_2O + K_2O (alkali content) is a measure of the feldspar content and also applicable for index of chemical maturity. The alkali content is between 2 and 7, with an average of 4 shows the presence of feldspars and low chemical maturity. The Fe_2O_3/K_2O ratio ranges from 2 to 21 (average=13); samples with low SiO_2/Al_2O_3 ratio and a higher Fe_2O_3/K_2O ratio should be mineralogically less stable and more prone to reactivity during supercritical CO_2 exposure (Farquhar et al., 2014); this is the case of the samples under investigation, thus they are mineralogically immature.

Colours are caused by presence of varying mixtures of mobile oxides such as haematite and limonite. Depletion of these oxides is mostly caused by weathering processes (Muhs et al., 1987). Al_2O_3/(CaO+MgO+Na_2O+K_2O) ratio can be used in determining the stability of mobile oxides as proposed by Gill and Yamane (1996). From the positive values obtained (0.12 to 1.71), it shows that there are stable mobile oxides in the Abeokuta Formation sandstone facies. The Presence of calcite is the most common cement in sandstone, although when present it does not fill all pore spaces completely but occurs as patchy cement. Calcite cemented sandstone often have their cement partially dissolved. It occurs as a result of chemical weathering of rocks (Hendry and Trewin, 1993). CaO+MgO/Al_2O_3 molecular weight ratio was used to determine calcification in the Abeokuta sandstone facies as proposed by Gills and Yamane (1996). All the samples have low values except Irolu 11 with a high value which indicates that the sandstones are less calcified.

An approach towards assessing detrital mineralogy is to use the Index of compositional variation (ICV) and ratio of K_2O/Al_2O_3 (Cox *et al.*, 1995). ICV is defined as:

(Fe_2O_3+Na_2O+CaO+MgO+TiO_2)/Al_2O_3. More matured sandstone with mostly clay minerals displays lower ICV values that are less than 1.0 and such sandstones are derived from cratonic environment (Cox et al., 1995). According to the results of the Index of Compositional Variation, all of the sandstones have values greater than 1; with Irolu 11 giving a much higher value (11.66). This shows that the sandstones are mineralogically immature.

Figure 9 shows the ratio of SiO_2/Al_2O_3 plotted against that of quartz / (feldspar + lithic fragments). Pettijohn (1975) interpreted these ratios to reflect the maturity of sandstones. Higher SiO_2 ratio coincides with higher silica phases of quartz, quartzite and chert which in turn reflects that such sandstones are mature (Al-Juboury, (2007). From Figure 9, the Abeokuta Formation sandstone facies exhibited low SiO_2 and are immature.

Table 3 shows the mineralogical composition of the samples: the quartz, feldspar and lithic (rock) fragments used to obtain the mineralogical maturity index (MMI), which was calculated using the parameters in Table 4 proposed by Nwajide and Hoque (1985). The mineralogical maturity index is determined using the expression:

$$MMI = \frac{\text{Proportion of Qtz}}{\text{Proportion of Fsp} + \text{Proportion of R. F}}$$

The MMI values range between 18 and 31.33 with an average of 22.4 suggesting the sediments to be sub mature to super mature.
The ZTR ratio (% of ultrastable zircon, rutile and tourmaline in the total non-opaque heavy mineral fraction) gives a measure of the degree of dissolution that has occurred (Hubert, 1962). The ZTR index was calculated using the percentage of the combined zircon, tourmaline and rutile grains for each sample according to the formula below referred to as Hubert's (1962) scheme:

.

$$\textbf{ZTR Index} = \frac{Zircon + Tourmaline + Rutile}{Total\ number\ of\ Non\ opaque\ heavy\ minerals}$$

This index is expressed in percentage and a measure of the maturity of a heavy mineral suite (Pettijohn et al., 1972). In greywackes and arkoses, the ZTR index is between 2-39%, and usually exceeds 90% in quartz arenites (Mange and Maurer, 1992). Accordingly, ZTR <75% implies immature to sub mature sediments and ZTR >75% indicates mineralogically matured sediments. According to Mange and Maurer (1992), the ZTR index values of between 75 and 88% are characteristics of mature sediments. The ZTR Index for the selected samples range from 63.33 to 76.92% with an average of 70.07%. Only one sample has ZTR index greater than 75%. Therefore, the ZTR indices suggest that nearly all the sediments are mineralogically immature to sub mature.

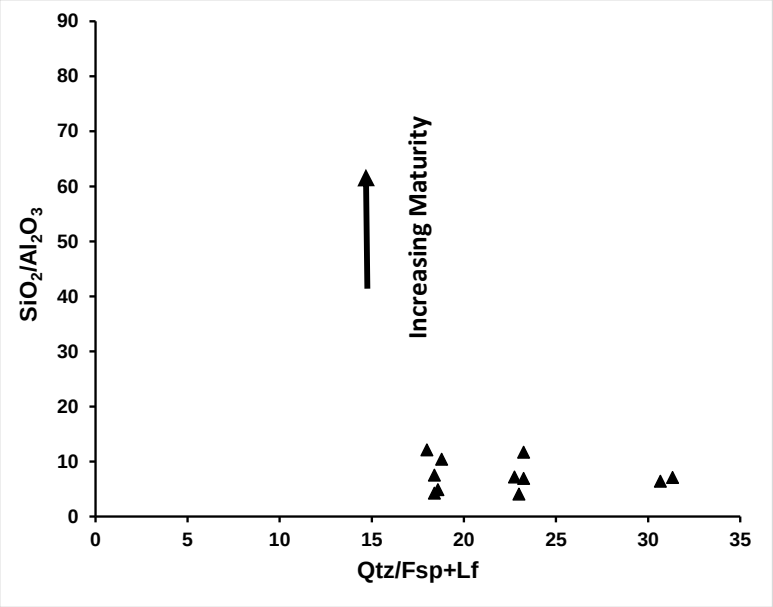

Figure 9. The ratio SiO_2/Al_2O_3 and Qtz/ (Fsp+Lf) (total quartz)/(feldspar + lithic fragments) in the Abeokuta sandstone facies. Adapted from Al-Juboury, (2007).

Table 3: Modal composition of the sandstone facies studied and the Mineralogical Maturity Index

Sample ID	**Quartz (Qtz)**	**Feldspar (Fsp)**	**Rock (Lithic) Fragment (RF)**	**Fsp+RF**	**% Qtz**	**% Fsp+RF**	**Mineralogical Maturity Index (MMI)**
Irolu 1	93	1	3	4	96	4	23.25
Irolu 2	92	2	3	5	95	5	18.40
Irolu 3	94	3	2	5	97	5	18.80
Irolu 5	92	2	3	5	95	5	18.40
Irolu 6	93	2	3	5	96	5	18.60
Irolu 7	91	1	3	4	94	4	22.75
Irolu 8	94	1	2	3	97	3	31.33
Irolu 9	92	1	2	3	95	3	30.67
Irolu 10	93	2	2	4	96	4	23.25
Irolu 11	90	2	3	5	93	5	18.00
Irolu 12	92	2	2	4	95	4	23.00
Average	**92.36**	**1.73**	**2.55**	**4.27**	**95.36**	**4.27**	**22.40**

Table 4: Maturity scale of Sandstone: Limiting % of Q and (F + RF) MI and maturity stage (Nwajide and Hoque, 1985).

Q =≥ 95% (F + RF) = 50%	MI = ≥ 19 Super mature
Q = 95-90% (F + RF) = 5-10%	MI = 19 - 9.0 Sub mature
Q = 90-75% (F + RF) = 10-25%	MI = 9.0-3.0 Sub mature
Q =75-50% (F + RF) = 25-50%	MI = 3.0-1.0 Immature
Q = < 50%	MI ≤ 1
(F + RF) > 50%	Extremely immature

Geochemistry

The results of the elemental distribution for the sandstone facies are presented in Table 2. The analyzed samples are dominated by SiO_2, which ranges from 43.83-71.66% (Av. 60.09%),

Silica enrichment is a measure of sandstone maturity, and is a reflection of the duration and intensity of weathering and destruction of other minerals during transportation (Lindsey, 1999). Silica enrichment also occurs by addition of silica cement, as quartz and opal (Lindsey, 1999). The variation of SiO_2 content is probably due to variation in grain size and diagenesis. Al_2O_3 ranges from 3.62-13.84% (Av. 8.95%) and is due to weathering effects. Fe_2O_3 ranges from 9.21-26.09% (Av. 16.14%) and according to Lindsey, (1999), the concentration of iron oxide (Fe_TO_3, total iron as Fe_2O_3) is the net result of provenance and processes that concentrate and preserve detrital ferromagnesian and iron minerals (mainly amphibole, mica, illite, ilmenite, and magnetite) and their alteration products (chlorite, hematite, and some clays). Concentration of detrital ferromagnesian minerals reflects their abundance in source rocks and is increased by hydraulic sorting and is decreased by chemical destruction during weathering and diagenesis under oxidizing conditions (Lindsey, 1999). CaO ranges from 0.42-28.88% (average 3.39); this might be due to dissolved diagenetic calcite cement. Harker diagrams are useful in comparing the abundances of the major oxides along a common axis. A decrease in the abundance of TiO_2, Fe_2O_3, CaO, Na_2O, MgO, MnO, K_2O, and Al_2O_3 as SiO_2 increases was not the trend observed (fig. 11), this could be due to sediment mixing.

The plot of SiO_2 vs Na_2O (Fig. 12) shows that there is a very low correlation with Na; the extrapolated regression equation did not pass through the origin, this being attributed to a small Na_2O contribution from the clay minerals.

There is a negative correlation between TiO_2 and $A1_2O_3$ (Fig. 13A), which may be as a result of depositional process and granulometry, this suggests that TiO_2 in the sandstone is not associated with phyllosilicates. $TiO_2/A1_20_3$ ratio is between 0.11 and 0.47 (av. 0.23). Spears & Kanaris-Sotiriou, (1975) showed that this ratio decreases as the grain size of the sediment decreases. This low value indicates that the sandstone matrix is composed of clay minerals.
There is positive correlation and linear relationship between K_2O and $A1_2O_3$ (Fig. 13B) as a result of changes in the quartz-matrix proportions, which according to Spears and Amin (1981) is due to grain-size-related quartz variations reflecting the grading.

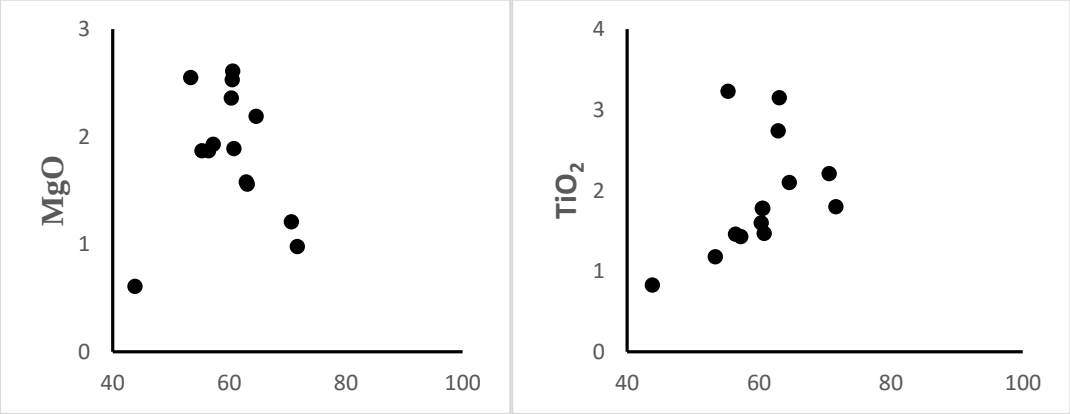

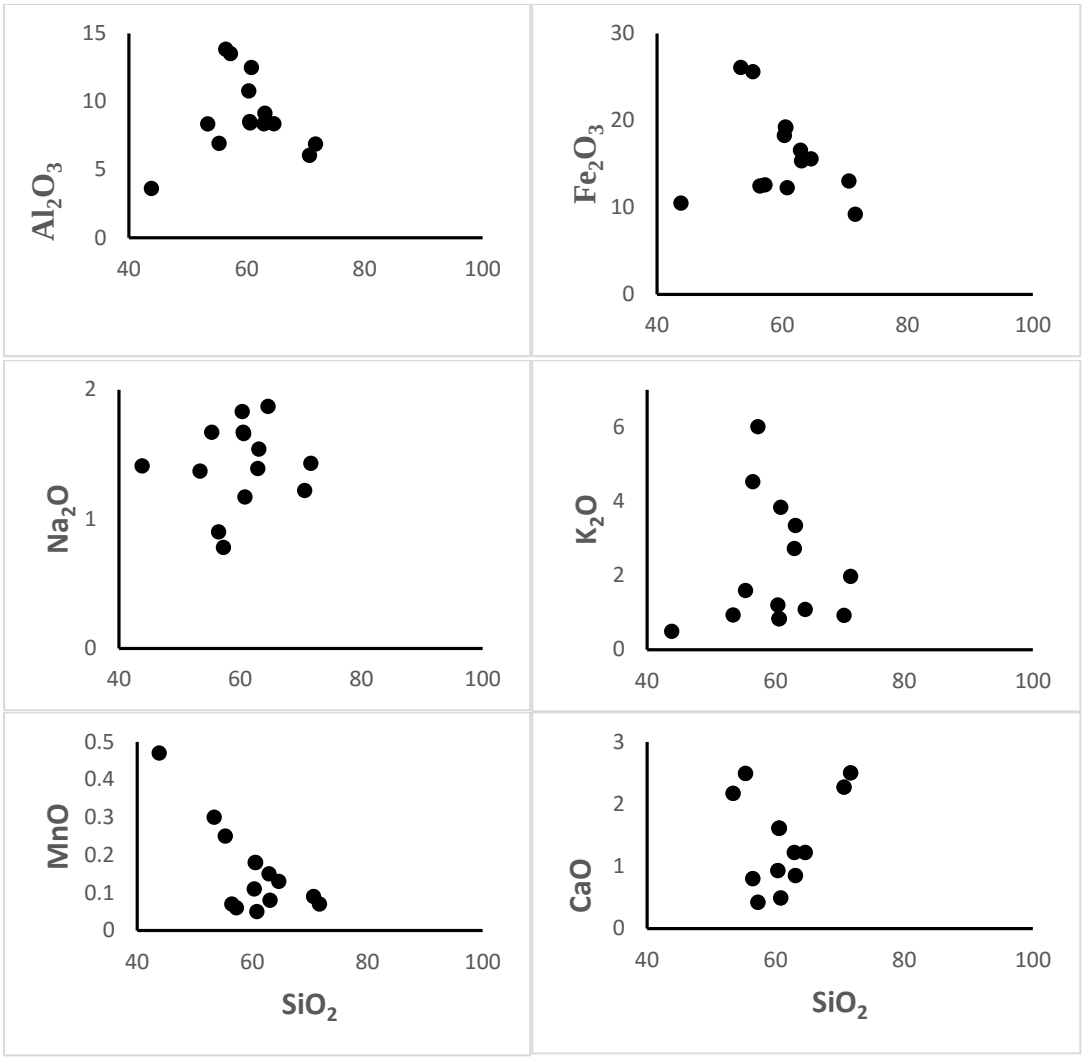

Figure 11. Harker diagram of major elements plotted against SiO_2 of the studied samples.

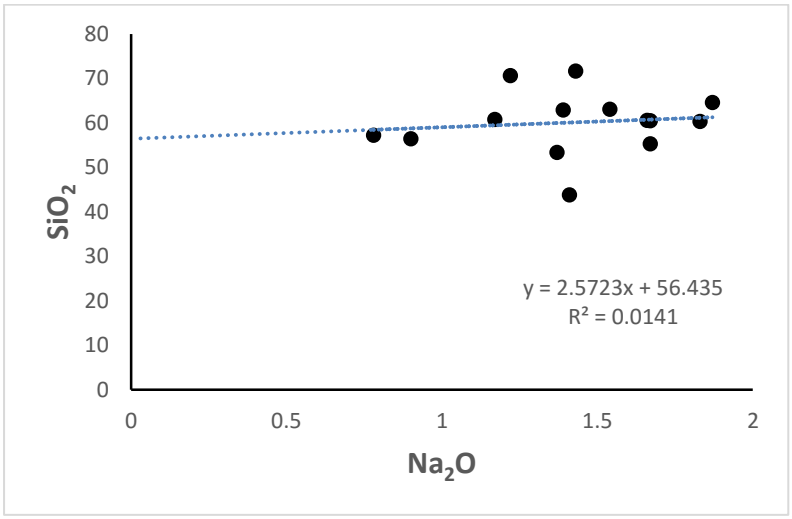

Figure 12. Plot of Na_2O against SiO_2, for the Abeokuta Formation

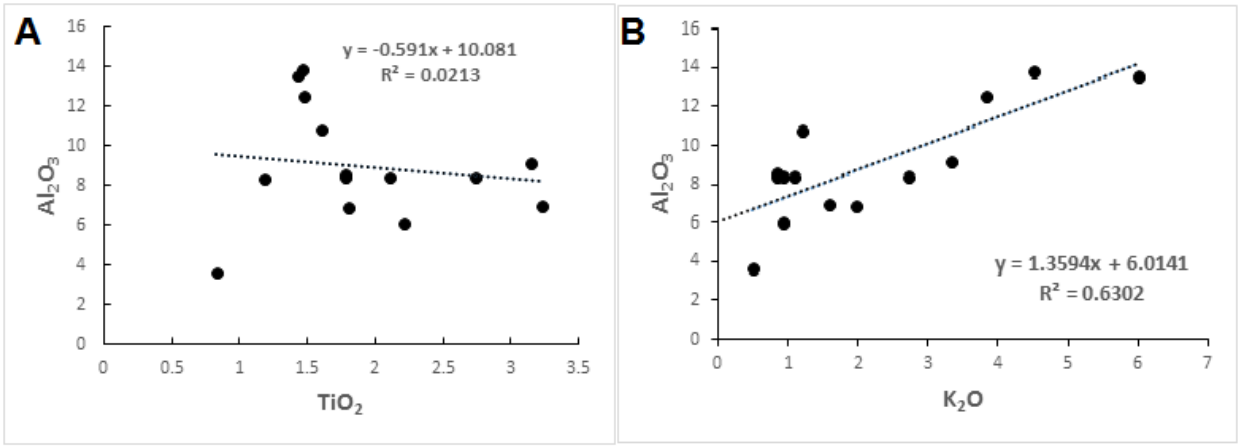

Figure 13. Correlation plots of (A) TiO_2 vs $A1_2O_3$ and (B) K_2O against $A1_2O_3$

K_2O is contained mainly by the clay minerals, a loss of K_2O associated with feldspar alteration produces a detectable scatter plot (Spears and Amin, 1981). As shown in Figure 14, there is a very weak correlation between K_2O and TiO_2 suggesting a loss of K_2O which is an indication of diagenetic alteration of feldspars.

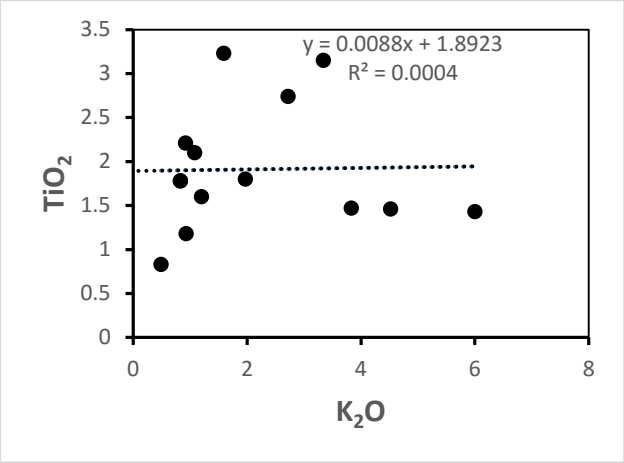

Figure 14. Correlation plot of K_2O and TiO_2

Arsenic concentration (102-330 ppm) is much higher than that for the UCC (4.8 ppm) which may be due to contamination. Ce, Cu, Pb, V, Y, Zn and Zr were enriched compared with the UCC and average sedimentary rocks (figure 16). The Abeokuta Formation sandstone is extremely depleted in REE (only Ce and Y present) due to the dilution effect of quartz. Zr, Ti, Nb, Hf and Y are preferentially partitioned into melts during fractional crystallization and anatexis (Feng and Kerrich, 1990), thus, they are enriched in felsic rather than mafic rocks. Co and Nb average values are close to the UCC values. Ba, Ni and Sr have average values lower than that of the UCC. Depletion of Ba may be due to leaching of barium from feldspar penecontemporaneous with feldspar dissolution (Schrijver et al., 1994).

In all the samples, Sr is strongly depleted except two with anomalous high values. Sr and Na are more mobile than Al, K, Rb, and Ba and consequently easily removed from parent rocks during chemical weathering (Yang et al., 2004). Depletion of Sr is more strongly related to feldspar weathering than to CaCO3 dissolving. The distribution of Sr during sedimentary processes is affected by strong adsorption on clay minerals. Strontium is easily mobilized

during weathering, especially in oxidizing acid environments, and is incorporated in clay minerals (Kovács, 2007). Figure 17 is a spidergraph of the trace and rare elements concentration of the Abeokuta formation.

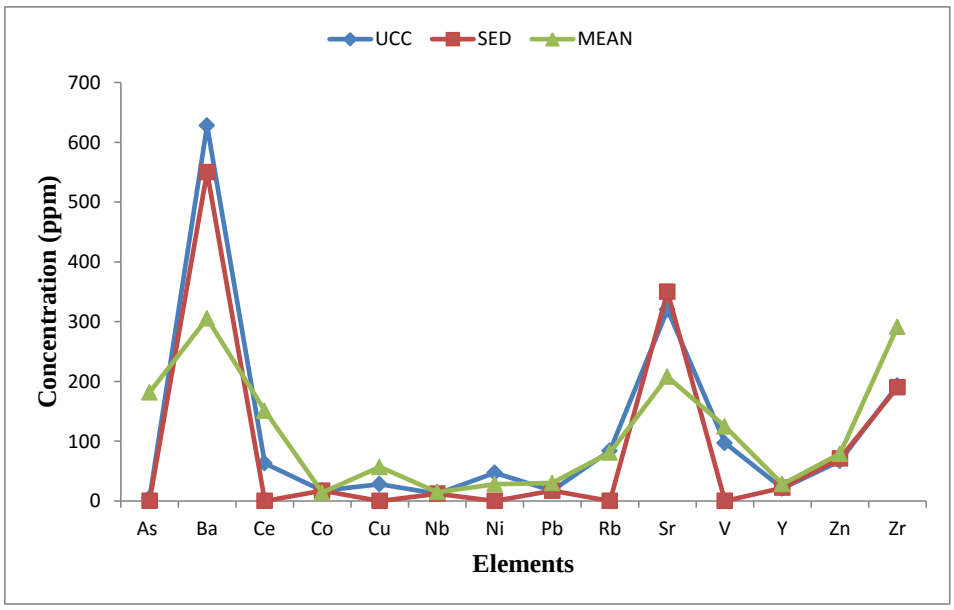

Figure 16. Spidergraph of the mean concentration of trace and rare elements in the sandstones relative to the UCC and SED. UCC= Upper Continental Crust data adapted from (Rudnick & Gao, 2003); SED. = sedimentary rocks data from (Ronov and Yaroshevsky, 1976; McLennan, 2001).

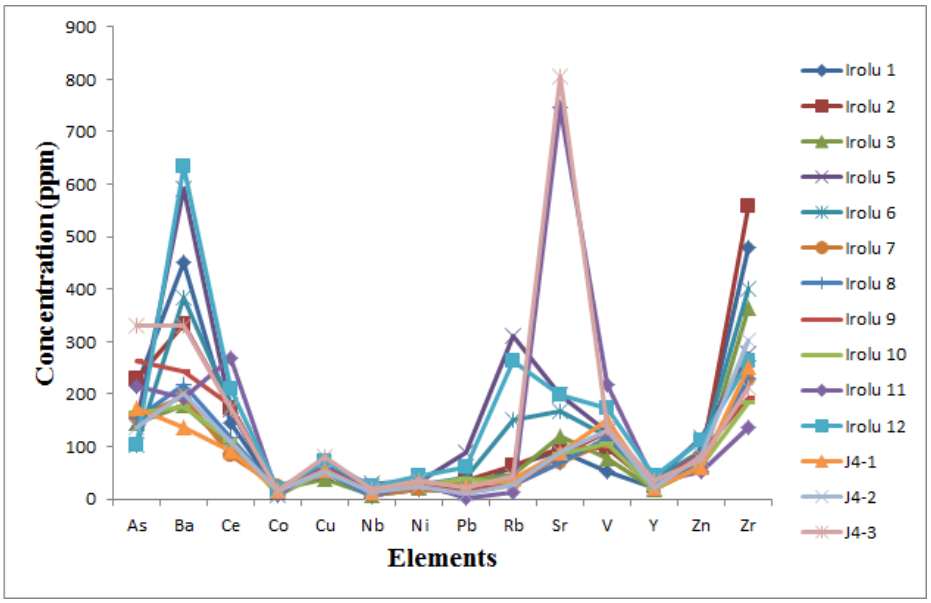

Figure 17. Spidergraph of the concentration of trace and rare elements in the sandstones

An average upper continental crust (UCC)-normalized spiderdiagram for the samples from the Abeokuta is shown in Figure 18. The insoluble residues are characterized by depletion in Ba, Sr, Ni, and enrichment in As, Zr and Ce relative to UCC. The irregularity of the plot patterns suggests the heterogeneity of the source. The UCC-normalized spiderdiagrams for mean samples values is shown in Figure 19, this also shows the marked enrichment of As and depletion of Ba, Sr and Ni.

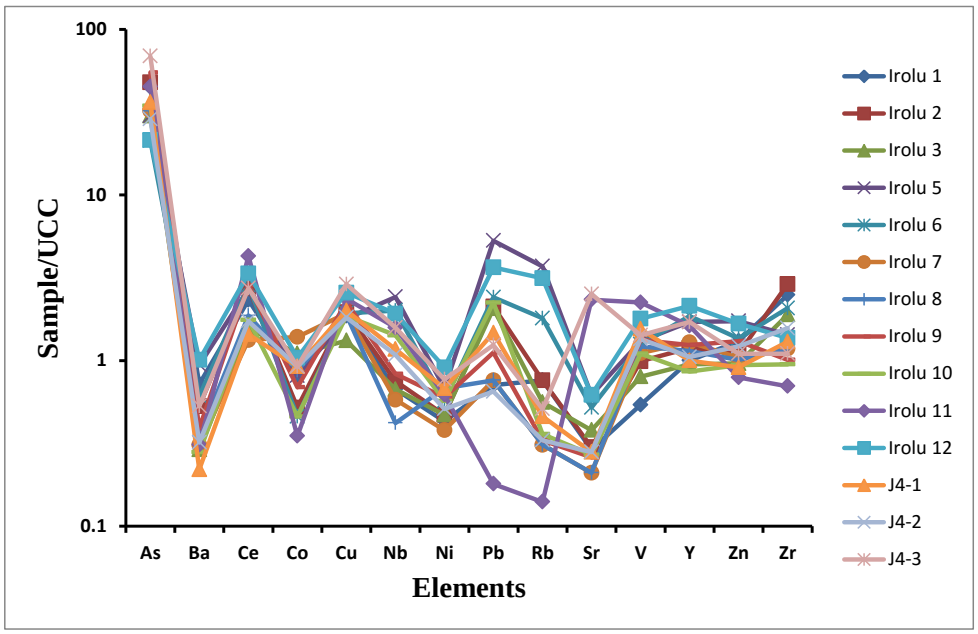

Figure 18. UCC-normalized spiderdiagrams for samples from the Abeokuta Formation.

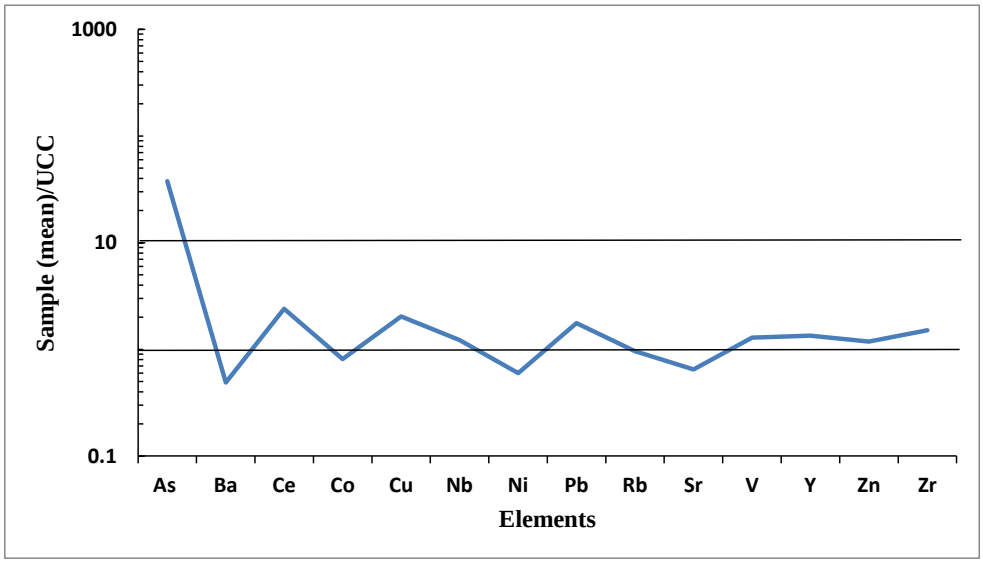

Figure 19. UCC-normalized spiderdiagrams for mean samples values from the Abeokuta Formation.

The Al—Ti—Zr ternary diagram monitors the effects of sorting processes (Garcia et al. 1994). On this diagram, mature sediments consisting of both sandstones and shales show a wide range of TiO2/Zr variations, whereas immature sediments of sandstones and shales show a more limited range of TiO2/Zr variations (Asiedu et al. 2000). On the Al—Ti—Zr diagram (Fig. 20), the Abeokuta Formation sandstones plotted in the CAS zone and outside all fields with a limited range of TiO2/Zr variations, suggesting poor sorting and rapid deposition of the studied sandstones.

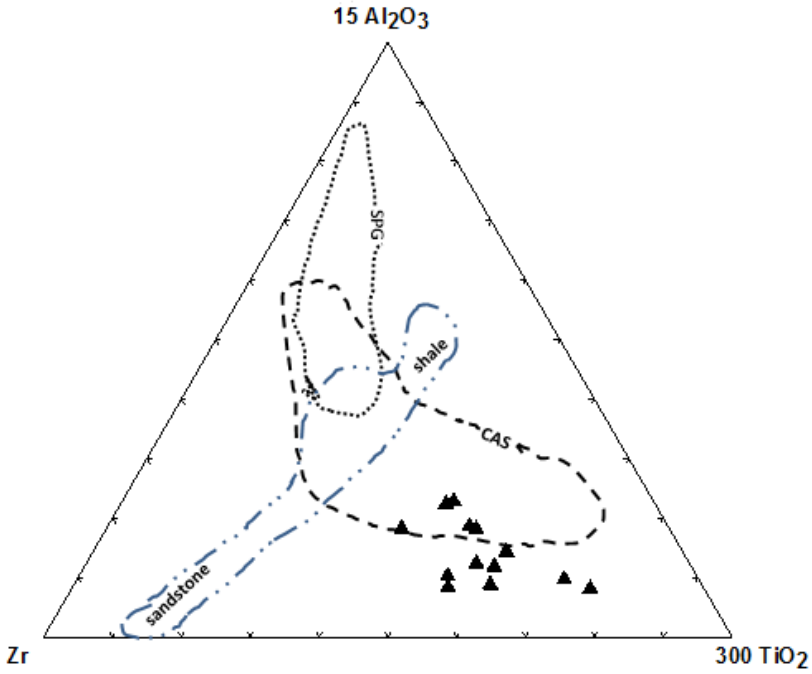

Figure 20. Al—Ti—Zr plot for the Abeokuta Formation sandstones. The solid contour refers to the observed range of compositions in clastic sediments. CAS refers to the fields of calc-alkaline suites and SPG refers to fields of strongly peraluminous granites (after Garcia et al. 1994).

CONCLUSIONS

The sandstone facies of the Abeokuta Formation exhibited varying classification nomenclatures using different classification schemes, which may be due to sediment supply from different sources. However, it is evident that the sandstones are rich in iron; are potassic and also rich in lithic materials. The sandstones can thus be classified as litharenites and sub-arkoses. The sandstones have a low SiO_2/Al_2O_3 value suggesting chemical immaturity; high degree of clayness and less calcified with stable mobile oxides. Index of compositional variation (ICV) values shows that the sandstones are mineralogically immature. The plot of ratio SiO_2/Al_2O_3 against quartz / (feldspar + lithic fragments) shows that the sandstones are immature. The ZTR indices suggest that nearly all the sediments are mineralogically immature to sub mature but mineralogical maturity index (MMI) suggests the sediments to be sub mature to super mature. A decrease in the abundance of TiO_2, Fe_2O_3, CaO, Na_2O, MgO, MnO, K_2O, and Al_2O_3 as SiO_2 increases was not the trend observed, this could be due to sediment mixing. Arsenic concentration is much higher than that for the UCC which may be due to contamination. Ce, Cu, Pb, V, Y, Zn and Zr were enriched compared with the UCC and average sedimentary rocks. Depletion of Sr is more strongly related to feldspar weathering than to CaCO3 dissolving. The Abeokuta Formation sandstone is extremely depleted in REE (only Ce and Y present) due to dilution effect of quartz. On the Al—Ti—Zr diagram, the sandstones plotted in the CAS zone and outside all fields with a limited range of TiO_2/Zr variations, suggesting poor sorting and rapid deposition.

REFERENCES

Al-Juboury A.I. (2007) Petrography and major element geochemistry of Late Triassic

Carpathian Keuper sandstones: Implications for provenance. *Bulletin de l'Institut Scientifique,* Rabat, section Sciences de la Terre, n°29, 1-14.

Asiedu D.K., Suzuki S., Nogami K. & Shibata T. (2000) Geochemistry of Lower Cretaceous sediments, Inner Zone of Southwest Japan: Constraints on provenance and tectonic environment. *Geochemical J.* 34, 155—173.

Bankole, et al. (2006) Palynostratigraphic Age and Paleoenvironments of the newly exposed section of the Oshosun Formation in the Sagamu Quarry, Dahomey Basin. *Nigerian Association of Petroleum Explorationists Bulletin.* vol. 19, 1 p. 25 – 30

Blatt, H., Middleton, G., & Murray, R., (1972) *Origin of sedimentary rocks*. Englewood Cliffs, New Jersey, Prentice-Hall, 634 p.

Farquhar, et al (2014) A fresh approach to investigating CO2 storage: Experimental CO_2-water-rock interactions in a low-salinity reservoir system, *Chemical Geology.* P. 1-70.

Feng, R., Kerrich, R. (1990) Geochemistry of fine-grained clastic sediments in the Archean Abitibi greenstone belt, Canada. Implications for provenance and tectonic setting. Geochimica Cosmochimica Acta, 54, 1061-1081.

Folk, R.L. (1974) *Petrology of Sedimentary Rocks*. Austin, TX, Hemphill Press, Second Edition, 182 p.

Garcia D., Fonteilles M. & Moutte J. (1994) Sedimentary fractionations between Al, Ti, and Zr and the genesis of strongly peraluminous granites. *J. Geol.* 102, 411—422.

Herron, M.M. (1988) Geochemical classification of terrigenous sands and shales from core or log data: *Journal of Sedimentary Petrology,* 58, p.820–829.

Hubert, J.F. (1962) A zircon-tourmaline-rutile maturity index and the interdependence of the composition of heavy mineral assemblages with the gross composition and texture of sandstones. *Journal of sedimentary petrology*, 32(3): 440-450.

Kovács, J. (2007) Chemical Weathering Intensity of the Late Cenozoic "Red Clay" Deposits in the Carpathian Basin. *Geochemistry International*, Vol. 45, No. 10, pp. 1056–1063.

Lindsey, D.A. (1999) An Evaluation of Alternative Chemical Classifications of Sandstones. *United State Geological Survey Open-File Report* 99-346, 23p.

Mange, M.A. & Maurer, F.W. (1992) *Heavy Minerals in Colour.* Chapman & Hall, London.

McLennan, S.M.. (2001) Relationships between the trace element composition of sedimentary rocks and upper continental crust: *Geochemistry Geophysics Geosystems*, v. 2, paper number 2000GC000109.

Nichols, G. (2009) *Sedimentology and stratigraphy* (2nd ed.). Wiley-Blackwell. Publishing, London, 419 pp.

Nigerian Geological Survey Agency, (2009) *Geological and mineral resources map of Ogun State , Nigeria.*

Nwajide, C.S., & Hoque, M. (1985) Problem of classification and maturity. Evaluation of a diagnostically altered fluvial Sandstone. *Geologic on Nujibouw*, vol.64, p. 67-70.

Pettijohn, F. J. (1963) Chemical composition of sandstones—excluding carbonate and volcanic sands, *in* Fleischer, M., ed., Data of Geochemistry, sixth edition, *U. S. Geological Survey Professional Paper 440-S*: 21 pp.

Pettijohn, F. J. (1975) *Sedimentary Rocks*, third edition: New York, Harper & Row: 628 pp.

Pettijohn, F.J., Potter, P.E., & Siever, R. (1972) *Sand and Sandstones*. New York, Springer-Verlag.

Potter, P.E. (1978) Petrology and chemistry of modern big river sands. *The Journal of Geology,* 86(4): 423–449.

Ronov, A.B., & Yaroshevsky, A.A. (1976) A New Model for the Chemical Structure of the Earth's Crust. *Geokhimiya*, No 12, pp. 1761-1795.

Roser, B. P., & Korsch, R. J. (1986) Determination of tectonic setting of sandstone-mudstone suites using SiO2 content and K2O/Na2O ratio. *J. Geol.*, 94, p.635-650.

Roser, et al (1996) Reconnaissance sandstone geochemistry, provenance, and tectonic setting of the lower Paleozoic terraines of the West Coast and Nelson, New Zealand. New Zealand. *J. Geol. Geophys.*, 39: 1-16.

Rudnick, R. L., & Gao, S. (2003) The Composition of the Continental Crust. In *Treatise on Geochemistry*. Elsevier–Pergamon, Oxford–London. Vol. 3, p. 1-64.

Schrijver, K., Zartman, R.E., & Williams-Jones, A.E. (1994): Lead and barium sources in Cambrian siliciclastics and sediment provenance of a sector of the Taconic Orogen, Quebec: a mixing scenario based on Pb-isotopic evidence. *Applied Geochemistry*, Volume 9, Issue 4, p.455-476.

Spears D.A. & Kanar1s-Sotiriou R. (1975) Titanium in some Carboniferous sediments from Great Britain. *Geochim. Cosmochim. Acta,* 40, 345-351.

Spears, D. A., & Amin, M. A. (1981) A Mineralogical and Geochemical Study of Turbidite Sandstones and Interbedded Shales, Mam Tor, Derbyshire, UK. *Clay Minerals*, 16, p. 333-345.

Wronkiewicz, D.J. and Condie, K.C., (1987): Geochemistry of Archean shales from the Witwatersrand Supergroup, South Africa: source-area weathering and provenance. Geochim. Cosmochim. Acta 51, pp. 2401–2416.

Yang, S. Y., Jung, H. S. and Li, C. X. (2004): Two Unique Weathering Regimes in the Changjiang and Huanghe Drainage Basins: Geochemical Evidence from River Sediments. Sediment. Geol. 164, p.19–34.